IEEE Access
Multidisciplinary ⋮ Rapid Review ⋮ Open Access Journal

Received February 15, 2020, accepted March 5, 2020, date of publication March 10, 2020, date of current version March 20, 2020.

Digital Object Identifier 10.1109/ACCESS.2020.2979871

Preamble Design and Detection for 5G Enabled Satellite Random Access

LI ZHEN[1], (Member, IEEE), TENG SUN[1], GUANGYUE LU[1], KEPING YU[2,3], (Member, IEEE), AND RUI DING[4]

[1]School of Communications and Information Engineering, Xi'an University of Posts and Telecommunications, Xi'an 710121, China
[2]Global Information and Telecommunication Institute, Waseda University, Tokyo 169-8050, Japan
[3]Shenzhen Boyi Technology Company, Ltd., Shenzhen 518125, China
[4]Institute of Telecommunication Satellite, China Academy of Space Technology, Beijing 100086, China

Corresponding authors: Keping Yu (keping.yu@aoni.waseda.jp) and Guangyue Lu (tonylugy@163.com)

This work was supported in part by the Natural Science Foundation of China (NSFC) under Grant 61901370, in part by the Special Research Project of Education Department of Shaanxi Province under Grant 19JK0794, in part by the Open Fund of the Shaanxi Key Laboratory of Information Communication Network and Security under Grant ICNS201801, in part by the Science and Technology Innovation Team of Shaanxi Province for Broadband Wireless and Application under Grant 2017KCT-30-02, and in part by Japan Society for the Promotion of Science (JSPS) Grants-in-Aid for Scientific Research (KAKENHI) under Grant JP18K18044.

ABSTRACT This paper deals with the crucial issue of random access (RA) preamble design and detection for fifth generation new radio (5G NR) enabled satellite communication systems. In consideration of the characteristics of satellite environment and system compatibility, a long preamble sequence is first constructed by cascading multiple different root Zadoff-Chu (ZC) sequences with large sub-carrier interval in time domain. Then, we further present a multiple sequence joint correlation (MSJC) based one-step timing detection scheme to effectively estimate the value of timing advance (TA), which is capable of flexibly adjusting the number of available ZC sequences involved in correlation operation. The superiority of the proposed method is mathematically validated in terms of robustness to carrier frequency offset (CFO), mitigation of noise, as well as computational complexity. Numerical results in a typical low-earth-orbit (LEO) based non-terrestrial network (NTN) scenario demonstrate that the proposed method, without the pre-compensation of timing and frequency offset, can achieve a remarkable timing performance improvement in comparison with the existing methods.

INDEX TERMS 5G, satellite communication, random access, preamble design, timing estimation.

I. INTRODUCTION

With the aim of service delivery in remote areas and improving service flexibility, it is predictable that satellite communication will become an indispensable component of the forthcoming fifth generation (5G) global networks. Ongoing activities and efforts are undertaken by 3rd generation partnership project (3GPP) to go deeper into the role of satellites in 5G new radio (NR) [1]. To this end, special attention should be paid to the unique characteristics of the satellite environment [2], and several crucial air interface technologies need to be modified to satisfy the satellite communication requirements [3], [17], in particular, the initial random access (RA) procedure between user equipment (UE) and satellite base station.

The associate editor coordinating the review of this manuscript and approving it for publication was Junfeng Wang.

As is well known, RA is mainly used for the establishment of the uplink connection from UE to base station in 5G NR [4]. When a UE attempt to access the network, it will select one of the available preambles to transmit on a RA time slot. If the base station successfully detects the presence of the transmitted preamble, the UE identity corresponding to this preamble will be determined, and its timing advance (TA) information, utilized to maintain the uplink synchronization, can also be acquired. It is obvious that effective design and detection of preamble sequence plays a pivotal role in the 5G RA procedure. Although there have been some related works in [5]–[8] with respect to this critical issue for terrestrial scenario, however, it may be unsuitable to remain adopting these methods in consideration of the characteristics of the satellite environment, such as longer prorogation distance, wider beam coverage, higher Doppler shift, and larger path loss. Consequently, a more reasonable design of RA preamble

and detection is undoubtedly required to cope with such noteworthy characteristics.

To be specific, there are several necessary improvements need to be highlighted. First, due to the longer prorogation distance and wider beam coverage, the RA preamble length should be significantly extended to tolerate the lager differential round trip delay, especially in the case that pre-compensation of timing offset is not performed at UE side. Such that, the longer cyclic prefix (CP) and guard interval (GT) is required to avoid the inter-symbol interference (ISI) between the adjacent frames, while the preamble sequence duration also needs to be increased on a large scale to guarantee the sufficient coverage. Next, the preamble detection method should work reliably under low received signal-to-noise ratios (SNRs), and have the robustness to large carrier frequency offset (CFO) for high-dynamic scenarios, e.g. low-earth-orbit (LEO) satellite communications. In addition, with the guarantee of an acceptable detection performance, a low-complexity timing estimator should be further considered to save the resource overhead for the load-limited satellite receiver. As aforementioned, effective design and reliable detection of RA preamble could be regarded as one of the predictable challenges for realizing the future 5G based satellite communication systems.

A. RELATIVE WORK

To tackle this challenge, several RA preamble design and detection methods for long term evolution (LTE)-satellite systems [9], [10] could be considered as reference, since the RA procedure in 5G systems is extremely similar to that in LTE systems. According to the general design principles in LTE [11], He *et al.* [12] utilized the difference of round trip delay to eliminate the time uncertainty within a satellite beam, so as to reduce both the durations of cyclic prefix (CP) and guard interval (GT). However, the sequence duration must be long enough to ensure the beam coverage performance, and thus a small sub-carrier spacing makes the preamble sequence vulnerable to carrier frequency offsets (CFOs). Another feasible solution is proposed by Li *et al.* [13] to construct the long sequence by cascading several same short Zadoff-Chu (ZC) sequences, but only fractional TA (normalized to the duration of short sequence) can be obtained, and additional preamble sequence needs to be resent for integral TA estimation. As an improvement in [14], we presented employing a single root ZC sequence with different cyclic shifts to constitute the long sequence, and jointly using all the correlation peaks for TA estimation, which can further enhance the access efficiency. Unfortunately, the fractional and integral TAs still need to be respectively estimated, and the residual CFO due to the oscillation instability will result in a reduction of TA estimation accuracy. There are also methods in [15] and [16] that took advantage of the conjugate symmetry of ZC sequences to cope with large CFOs. Although better timing estimation performance is achieved in the presence of integral CFO (normalized to the sub-carrier interval), both methods will suffer from a distinct performance degradation if the fractional CFO exists. Moreover, the extra utilization of transmission resources leads to high implementation complexities that are hard to bear for the load-limited satellite receiver.

Recently, 3GPP has discussed some possible solutions for RA preamble design in 5G NR enabled non-terrestrial network (NTN) [17]. With assumption on pre-compensation of timing and frequency offset, it is suggested that the existing 5G RA preamble formats and sequences can be reused. However, if pre-compensation of timing and frequency offset is not performed at UE side, RA preamble formats and sequences should be redesigned based on enhanced ZC sequence or Gold/m-sequence. By employing ZC sequence, there are two major advanced ideas: one is to repeatedly cascade of a single root ZC sequence with larger sub-carrier interval, which can be detected by the method proposed in [13]; the other is to cascade two different root long/repeated ZC sequences that can eliminate the influence of integral CFO. For Gold/m-sequence based preamble sequence, the additional processing procedure is essential, e.g., modulation and transform precoding.

B. CONTRIBUTION

In light of the 5G application requirements, the 5G enabled satellite communication system is expected to be capable of forcefully ensuring availability, reliability and robustness without a degradation in performance or an increment in cost [18]. Nevertheless, the unique and intricate satellite communication environment presents considerable challenges to satisfy this target in the real sense, especially for the core RA technology in satellite air interface. In this paper, we focus attention on the design of a more robust RA preamble and the corresponding timing detection detection scheme without the pre-compensation of timing and frequency offset, and the main contributions of our paper are summarized as follows:

- By taking into account the system compatibility and peculiarities of satellite environment, a novel preamble sequence, named as multiple root-cascading long sequence (MR-CLS), is constructed by concatenating a series of different short root ZC sub-sequences in time domain. Such that, the preamble sequence not only can cope with the wide coverage and time uncertainty within a satellite beam, but also has a relatively large sub-carrier interval.
- For achieving a reliable TA estimation performance at the presence of large CFOs and low received SNRs, while considering the construction characteristics of MR-CLS, we first propose a multiple sequence joint correlation (MSJC) based timing metric for power delay profile (PDP) computation. The key idea is to reconstruct the local sequence and the received sequence by flexibly changing the composition of their sub-sequences, and perform the length-varying sliding correlation between the constructed two sequences instead of the traditional periodical correlation to obtain PDP. Further, we theoretically derive the peak extraction threshold according to the target probability of false alarm,

by the statistical analysis of the timing metric at the wrong timing position. Finally, the value of TA can be directly obtained in one-step timing estimation, and consequently is conducive to improving the access efficiency compared to the state-of-the-art schemes in [13] and [14].

- Though statistical analyzing the proposed method in case of a full-sequence pattern match, we have demonstrated that our method can essentially eliminate the adverse impact of CFO on the timing detection, and is able to obtain a much better noise-mitigation capability by increasing the available sub-sequences involved in PDP calculation. Moreover, a low-complexity timing function is also presented to enhance the computational efficiency of preamble detection for the load-limited satellite receiver.
- Simulation results under a typical satellite line-of-sight (LoS) channel indicate the validity of mathematical analysis. It is shown that the proposed method can significantly improve the timing detection performance in terms of mean square error (MSE) and error detection probability (EDP), compared with the previous methods.

The rest of this paper is organized as follows. Section II is dedicated to the RA preamble design in satellite environments, wherein a new preamble MR-CLS is presented and its signal model is described. In Section III, the corresponding timing detection method based on MSJC is further proposed from the aspects of PDP calculation, correlation peak detection, and TA estimation. The performance of the proposed method is theoretically and numerically assessed in Section IV and Section V, respectively. Finally, Section VI concludes the paper.

II. RANDOM ACCESS PREAMBLE DESIGN

Generally, random access (RA) preamble has a unified signal format, which is made up of three components: sequence (SEQ), cyclic prefix and guard time. We denote the duration of each component as T_{SEQ}, T_{CP}, and T_{GT}, respectively. Note that, CP can address the time uncertainty and multipath delay spread, so as to ensure the sequence integrity of the received RA preamble in the observation window, while GT is used to absorb the propagation delay and avoid ISI. Hence, their durations, T_{CP} and T_{GT}, can be both represented as the maximum value of the difference of round trip delay within the cell. Besides, the duration of SEQ, T_{SEQ}, is closely related to cell coverage, and a longer sequence stands for a wider coverage. For preamble sequence, ZC sequence has been extensively adopted to generate preamble sequences due to its perfect auto-correlation properties and low peak-to-average power ratio, and can be given by $ZC\,[n] \triangleq \exp\left[-j\pi un\,(n+1)/N_{zc}\right]$ for $n = 0, \ldots, N_{zc}-1$, where $u \in \{1, \ldots, N_{zc}-1\}$ denotes the number of root and N_{zc} is the length of sequence.

According to the 3GPP technical specification [4], various preamble formats have been provided for different terrestrial cell scenarios, in which the maximum radius that can be supported is only 100 km and the corresponding T_{SEQ} is 0.8 ms. It is worth noting that, compared with the terrestrial scenarios, the satellite communication system usually has a wider coverage range and longer propagation time delay. Such that, the existing RA preamble formats cannot satisfy the access performance requirements in satellite scenarios, and consequently, T_{SEQ} is necessary to be redesigned. Taking the S-band LEO1200 based NTN scenario [17] as an example (the detailed system parameters can be seen in Table 1), it can be found that the maximum differential round-trip delay difference could reach to be 3.4 ms. Further, the satisfied T_{SEQ} is calculated as 6.4 ms from link budget [11], which becomes 8 times of that of terrestrial one. That is to say, the preamble duration should be remarkably extended to provide adequate beam coverage.

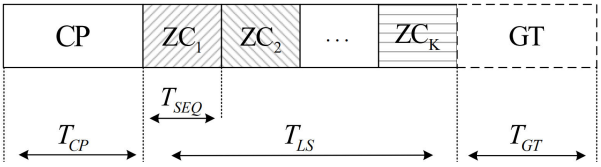

FIGURE 1. Preamble structure of the proposed MR-CLS.

In order to satisfy the duration requirements in the satellite environment, Li *et al.* [13] presented to construct the preamble sequence by cascading the same root ZC sequences used in terrestrial scene. However, at the receiver, by utilizing the local root ZC sequence to detect the transmitted sequence, the non-unique correlation peaks will emerge in the detection window, so that only the normalized fractional TA can be determined; then another sequence needs to be sent for the estimation of integral TA. By considering the long prorogation distance between the satellite and the user, this method undoubtedly increases both the user access delay and signaling overhead. For further improving the access efficiency, we propose to create a long preamble sequence, named as multiple root-cascading long sequence (MR-CLS), by concatenating a series of different short root sequences in time domain, as illustrated in Fig. 1. Here the long preamble sequence is composed of K short different ZC root sequences with the duration T_{SEQ}, namely, the duration of the long preamble sequence, T_{LS}, is equal to KT_{SEQ}. It is obvious that, the proposed long sequence can not only reuse terrestrial preamble sequence format with large sub-carrier interval, but also satisfy the requirement of coverage performance within a satellite beam.

Based on the sequence format in Fig. 1, without loss of generality, the signal model of MR-CLS can be formulated as

$$\mathbf{S} = [\mathbf{s_1}, \ldots, \mathbf{s_K}] \tag{1}$$

where the sub-vector $\mathbf{s_l} = \mathbf{ZC_l}$ represents the lth short ZC sequence with length of N_{zc}, and the corresponding root index is u_l for $l = 1, \ldots, K$. It should be noted that, thanks to the minimum cross-correlation property of ZC sequence, when using any local root ZC sequence for timing detection, only a

unique correlation peak will appear in the detection window. That is to say, the utilization of the proposed MR-CLS can directly acquire the accurate TA value though one-step timing detection, which is significantly conducive to improving the access efficiency.

If a user within the beam initiates random access request, it will randomly select a local long sequence as the preamble sequence to send. When the transmitted sequence passes through a typical satellite line-of-sight (LoS) channel, the sample of the received signal can be expressed as

$$R(n) = \rho S(n-\tau)\, e^{\frac{j2\pi\varepsilon n}{KN_{ZC}}} + w(n), \quad 0 \le n \le KN_{ZC} - 1 \tag{2}$$

where ρ, τ, ε, $S(n)$, $w(n)$ denote the channel gain, the propagation delay, the normalized CFO to the sub-carrier interval, the sample of the transmitted preamble sequence, and complex additive white Gaussian noise (AWGN) with the mean zero and variance σ_w^2, respectively.

III. ROBUST TIMING DETECTION BASED ON MR-CLS

In this section, by employing the proposed long sequence MR-CLS, we focus on the design of the corresponding timing detection method from the aspects of power delay profile (PDP) calculation, correlation peak detection, and TA estimation.

A. PDP CALCULATION

With the aim of achieving a reliable timing estimation performance at low received SNRs and the presence of large CFOs, while considering the construction characteristics of MR-CLS, we first propose a multiple sequence joint correlation (MSJC) based timing metric for PDP computation. The main idea of the proposed method is to reconstruct the local sequence and the received sequence by flexibly changing the composition of their sub-sequences, and perform length-varying sliding correlation between the constructed two sequences instead of traditional discrete time-domain periodical correlation to obtain the power delay profile.

Let $\mathbf{S_m}=\left[\mathbf{s_{m,1}}, \ldots, \mathbf{s_{m,K}}\right]$ be the shifted vector obtained from cyclic shifting the transmitted sequence $\mathbf{S}=[\mathbf{s_1}, \ldots, \mathbf{s_K}]$ by m times of N_{zc}, i.e. $\mathbf{S_m} = circshift(\mathbf{S}, mN_{ZC})$ for $m \in \{1, K-1\}$, where $circshift(\cdot)$ is the cyclic shift operator, and the reconstructed local vector can be denoted as

$$\mathbf{a_m} = \left[\mathbf{a_{m,1}}, \ldots, \mathbf{a_{m,K}}\right], \tag{3}$$

where the lth local sub-vector is expressed as $\mathbf{a_{m,l}} = \mathbf{s_l^*} \circ \mathbf{s_{m,l}}$ for $l \in \{1, \ldots, K\}$, $(\cdot)^*$ denotes the complex conjugate operation, and $\circ$ is the Hadamard product that represents the element by element multiplication of the two vectors. Similarly, the received sequence and its cyclic shift sequence at the timing index d are represented as $\mathbf{R^d}=\left[\mathbf{r_1^d}, \ldots, \mathbf{r_K^d}\right]$ and $\mathbf{R_m^d}=\left[\mathbf{r_{m,1}^d}, \ldots, \mathbf{r_{m,K}^d}\right]$, respectively. We reconstruct the received vector in terms of K sub-vectors as follows

$$\mathbf{b_m^d}=\left[\mathbf{b_{m,1}^d}, \ldots, \mathbf{b_{m,K}^d}\right], \tag{4}$$

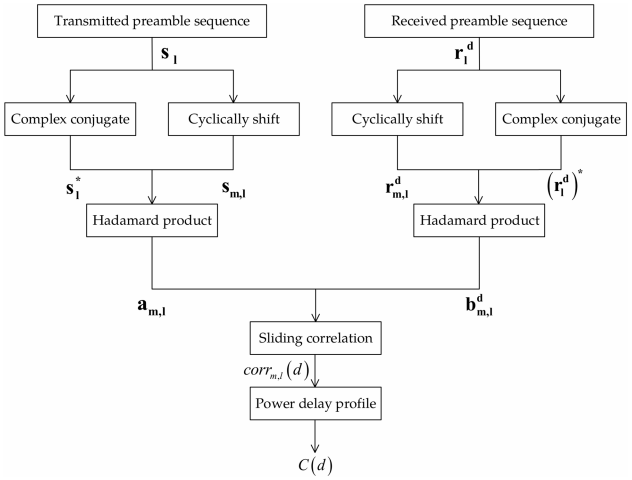

FIGURE 2. PDP calculation procedure based on the proposed MSJC.

where the lth received sub-vector is given by $\mathbf{b_{m,l}^d}=\left(\mathbf{r_l^d}\right)^* \circ \mathbf{r_{m,l}^d}$.

As shown in Fig. 2, the PDP calculation procedure based on the proposed MSJC is specifically described as follows: first of all, the lth sub-sequence $\mathbf{s_l}$ of MR-CLS is cyclically shifted by m times of N_{zc} to get $\mathbf{s_{m,l}}$; further, the Hadamard product operation between $\mathbf{s_l^*}$ and $\mathbf{s_{m,l}}$ is performed to generate the reconstructed local sequence, named as $\mathbf{a_{m,l}}$, i.e., $\mathbf{a_{m,l}} = \mathbf{s_l}^* \circ \mathbf{s_{m,l}}$; meanwhile, at the timing index d, the lth received sub-sequence $\mathbf{r_l^d}$ of $\mathbf{R^d}$ is transformed according to the format of $\mathbf{a_{m,l}}$ to obtain the reconstructed received sequence $\mathbf{b_{m,l}^d}$, namely, $\mathbf{b_{m,l}^d} = \left(\mathbf{r_l^d}\right)^* \circ \mathbf{r_{m,l}^d}$; then, by leveraging the sliding correlation between the two reconstructed sequences $\mathbf{a_{m,l}}$ and $\mathbf{b_{m,l}^d}$, the correlation result, $corr_{m,l}(d)$, is achieved as

$$corr_{m,l}(d) = \mathbf{a_{m,l}^*}\left(\mathbf{b_{m,l}^d}\right)^{\top}; \tag{5}$$

finally, the normalized PDP, $C(d)$, can be determined by accumulating all the correlation results and multiplying the corresponding normalization coefficient, which can be given by

$$C(d) = \frac{1}{N_{zc}ML}\sum_{m=1}^{M}\sum_{l=1}^{L}\left|corr_{m,l}(d)\right|, \tag{6}$$

where $M \in \{1, \ldots, K-1\}$ denotes the time of cyclic shifts and $L \in \{1, \ldots, K\}$ is the total number of the used sub-sequences.

B. PEAK DETECTION

For effective TA estimation, it is expected that the correlation peak at the correct timing point should be lager than a predefined detection threshold, while the other values of PDP at the wrong timing points below this threshold. Accordingly, the reliable detection threshold could be determined on the basis of the required false alarm probability of the satellite receiver, which can be defined as the probability that the PDP value exceeds the threshold when no RA preamble is transmitted. Next, through analyzing the statistical properties

of the timing metric at the wrong timing position, we concentrate on designing the detection threshold corresponding to the target probability of false alarm.

At the wrong timing index d_f, the received signal in (2) only contains the noise term, i.e., $R(d_f) = w(d_f)$. In this case, submitting (2) to (6), the PDP function $C\left(d_f\right)$ can be described as

$$\begin{aligned} & C\left(d_f\right) \\ &= \frac{\sum_{m=1}^{M}\sum_{l=1}^{L}\left|corr_{m,l}\left(d_f\right)\right|}{N_{zc}ML} \\ &= \frac{\sum_{m=1}^{M}\sum_{l=1}^{L}\left|\sum_{n=0}^{N_{zc}-1} a_{m,l}^{*}\left(n\right) b_{m,l}\left(n+d_f\right)\right|}{N_{zc}ML} \\ &= \frac{\sum_{m=1}^{M}\sum_{l=1}^{L}\left|\sum_{n=0}^{N_{zc}-1} ZC_l(n)ZC_{m,l}^{*}(n)\, w_l^{*}\left(n+d_f\right) w_{m,l}\left(n+d_f\right)\right|}{N_{zc}ML} \end{aligned} \tag{7}$$

Since $\left|ZC_l\left(n\right)ZC_{m,l}^{*}\left(n\right)\right|$ is equal to 1 always holds, $ZC_l\left(n\right)ZC_{m,l}^{*}\left(n\right)$ can be represented as a exponential form so that each term in (7) is virtually the phase rotation of $w_l^{*}\left(n+d_f\right)w_{m,l}\left(n+d_f\right)$, and thus it suffices to inspect its distribution. By considering the fact that $w_l^{*}\left(n+\tau\right)$ and $w_{m,l}\left(n+d_f\right)$ are independent and identically distributed (i.i.d.) complex Gaussian random variables with mean zero and variance σ_w^2, it can be known in Appendix that $corr_{m,l}\left(d_f\right)$ approximately obeys a complex Gaussian distribution with mean zero and variance $N_{zc}\sigma_w^2$. Hence we can obtain that $\left|corr_{m,l}\left(d_f\right)\right|$ is a Rayleigh random variable, and its mean and variance are expressed as

$$E\left\{\left|corr_{m,l}\left(d_f\right)\right|\right\} = \sqrt{\frac{\pi}{4}N_{zc}}\sigma_w \tag{8}$$

and

$$Var\left\{\left|corr_{m,l}\left(d_f\right)\right|\right\} = \frac{4-\pi}{4}N_{zc}\sigma_w^2, \tag{9}$$

where $E\{\cdot\}$ and $Var\{\cdot\}$ denote the operators of expectation and variance, respectively.

Note that in (7), $C\left(d_f\right)$ can be regarded as the summation of $M \times L$ i.i.d. Rayleigh random variables. In this case, the probability of false alarm, P_{FA}, which is defined as the probability that the PDP function at the wrong timing index exceeds the preset threshold β, is given by

$$\begin{aligned} P_{FA} &= P\left(C\left(d_f\right) > \beta\right) \\ &= P\left(\frac{1}{N_{zc}ML}\sum_{m=1}^{M}\sum_{l=1}^{L}\left|corr_{m,l}\left(d_f\right)\right| > \beta\right). \end{aligned} \tag{10}$$

However, the probability distribution of the sum of Rayleigh random variables with any dimension does not have a closed-form solution [19], [20]. That is to say, it is arduous to derive out the exact distribution of the PDP function at the wrong timing position, which also brings difficulties to the determination of the detection threshold. Consequently, we propose to utilize the properties of probability inequality [21] to solve this problem, i.e.

$$P_{FA} \le \sum_{m=1}^{M}\sum_{l=1}^{L} P(|corr_{l,m}(d_f)| > N_{zc}\beta). \tag{11}$$

According to the probability density function (PDF) of Rayleigh random variable, (11) can be further derived as

$$\begin{aligned} P_{FA} &\le \sum_{m=1}^{M}\sum_{l=1}^{L}\exp[-(N_{zc}\beta)^2/Var\{corr_{l,m}(d_f)\}] \\ &= ML\exp[-N_{zc}\beta^2/\sigma_w^2]. \end{aligned} \tag{12}$$

Let $P_{FA_{\max}}$ be the allowable maximum probability of false alarm, then we have

$$P_{FA_{\max}} = ML\exp[-N_{zc}\beta^2/\sigma_w^2]. \tag{13}$$

It is noteworthy from (13) that the detection threshold β can be obtained with regard to a given $P_{FA_{\max}}$ for RA preamble detection, and is determined as

$$\beta = \sqrt{\frac{-\sigma_w^2\ln\left(P_{FA_{\max}}/ML\right)}{N_{zc}}}. \tag{14}$$

C. TA ESTIMATION

Based on the aforementioned derivation of detection threshold, the desirable value of TA can be finally obtained as follows:

$$\hat{d} = \arg\max_{d}\left\{C\left(d\right) > \beta\right\}, \tag{15}$$

where $\hat{d}$ denotes the correct timing index that means a full-sequence pattern match between the received preamble and its local version, which can be determined by searching the maximum PDP peak that exceeds the given detection threshold. Note that, for achieving a reliable timing estimation, β can be flexibly adjusted according to the target probability of false alarm, the time of cyclic shifts, and the number of the used sub-sequences.

In order to further demonstrate the estimation accuracy of the proposed method, Fig. 3 depicts the PDP curve based on MSJC in a typical LEO based NTN scenario, where SNR, τ, and ε are set as -12 dB, 3000 samples, and 10.5, respectively. In addition, the total number of sub-sequences K is set as 8, the cyclic shift offset is N_{zc}, and the number of short sequences utilized in PDP calculation is 8. It can be observed from Fig. 3 that, at the correct timing detection position, there exists a unique impulse-like correlation peak larger than the predefined threshold without position offset and energy leakage, which can effectively indicate the start of the received preamble sequence. That is to say, the proposed method can be applied to the satellite LoS channel with a strong main diameter. Moreover, compared with the timing detection method in [13] and [14], the proposed scheme can

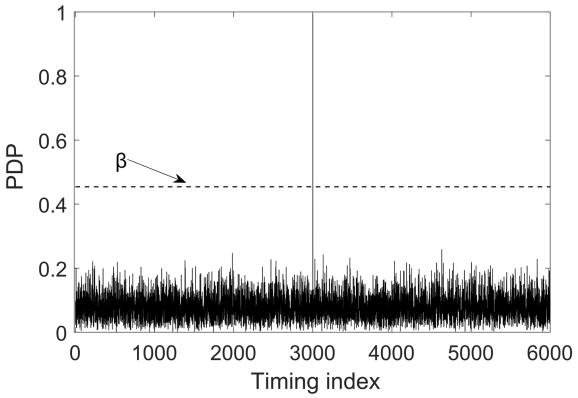

FIGURE 3. An illustration of the proposed timing estimation in a typical LEO based NTN scenario.

directly determine the value of TA in one-step detection, and consequently also improves the access efficiency.

IV. PERFORMANCE EVALUATION AND DISCUSSIONS

In order to reveal the suitability of the proposed timing detection method in satellite environments, we further assess its performance in terms of robustness to CFO, mitigation of noise, as well as computational complexity.

A. ROBUSTNESS TO CFO

As analyzed in [25] and [26], ZC sequence has been verified to be sensitive to CFO for orthogonal frequency division multiplexing (OFDM) systems, and thus large CFOs will lead to severe performance degradation in timing estimation. It should be mentioned that, for non-geostationary earth orbit (NGEO) satellite communication systems, the maximum value of CFO can reach to be even more than 40 KHz [17], [27], in which case the RA preamble detection method must have the capability of resisting to large CFOs. In the following, we reveal the influence of CFO on the correlation peak for the proposed MSJC.

At the correct detection position, i.e., $\hat{d} = \tau$, the correlation function can reach to be its maximum, by submitting (1) and (2) to (5), it can be rewritten as

$$\begin{aligned} corr_{m,l}(\tau) = & \sum_{n=0}^{N_{zc}-1} ZC_l(n)\, ZC_{m,l}{}^*(n) \\ & \times \left(\rho^* ZC_l^*(n)\, e^{\frac{-j2\pi\varepsilon(n+\tau)}{KN_{zc}}} + w_l^*(n+\tau)\right) \\ & \times \left(\rho ZC_{m,l}(n)\, e^{\frac{j2\pi\varepsilon(n+mN_{zc}+\tau)}{KN_{zc}}} + w_{m,l}(n+\tau)\right). \end{aligned} \tag{16}$$

Since the phase rotation of noise does not affect its probability distribution, $corr_{m,l}(\tau)$ can be further given by

$$corr_{m,l}(\tau) = e^{\frac{j2\pi\varepsilon m}{K}}\left(P_{m,l} + Q_{m,l} + X_{m,l} + W_{m,l}\right), \tag{17}$$

where $P_{m,l}$, $Q_{m,l}$, $X_{m,l}$, and $W_{m,l}$ are respectively represented as

$$P_{m,l} = \sum_{n=0}^{N_{zc}-1} |\rho|^2 |ZC_l(n)|^2 |ZC_l(n+mN_{zc})|^2, \tag{18}$$

$$Q_{m,l} = \sum_{n=0}^{N_{zc}-1} \rho^* |ZC_l(n)|^2 ZC_{m,l}(n)\, w_{m,l}(n+\tau), \tag{19}$$

$$X_{m,l} = \sum_{n=0}^{N_{zc}-1} \rho ZC_l^*(n) |ZC_{m,l}(n)|^2 w_l^*(n+\tau), \tag{20}$$

$$W_{m,l} = \sum_{n=0}^{N_{zc}-1} ZC_l(n)\, ZC_{m,l}^*(n)\, w_{m,l}(n+\tau)\, w_l^*(n+\tau). \tag{21}$$

It can be observed from (17) that the impact of CFO on the correct detection peak eventually becomes a constant term, that is $e^{j2\pi\varepsilon m/K}$. In this case, by taking the modulus operation of $corr_{m,l}(\tau)$, this term is equal to one, which means that CFO has no effect on the correlation $|corr_{m,l}(d)|$ and the PDP $C(d)$ at the correct timing index. Thus, we can obtain that the proposed MSJC is capable of achieving the robustness to large CFOs.

B. MITIGATION OF NOISE

The mitigation of noise is also an important issue to be considered in timing detection. It is clear from (19), (20), and (21) that $Q_{m,l}$, $X_{m,l}$, $W_{m,l}$ are affected by noise. By deriving the probability distribution of these three terms in the following, the anti-noise capability of the proposed MSJC can be revealed. For convenience, we primarily concern with the case that a fixed cyclic shift is employed.

It should be noted that the complex random variables $Q_{m,l}$ and $X_{m,l}$ are composed of mutually independent noise terms. Due to the constant envelope property of ZC sequence, i.e. $|ZC_l(n)|^2 = \left|ZC_{m,l}(n)\right|^2 = 1$, and thus we can obtain that $Q_{m,l}$ and $X_{m,l}$ are both complex Gaussian random variables with mean zero and variance $N_{zc}|\rho|^2\sigma_w^2$. Note that $w_l(n+\tau+mN_{zc})$ and $w_l(n+\tau)$ are independent of each other, $Q_{m,l} + X_{m,l}$ is still a complex Gaussian random variable with mean zero and variance $2N_{zc}|\rho|^2\sigma_w^2$. Since $\left|ZC_l(n)\, ZC_{m,l}^*(n)\right| = 1$ always holds, $ZC_l(n)\, ZC_{m,l}^*(n)$ can be expressed in the exponential form so that each term in $W_{m,l}$ is the phase rotation of $w_{m,l}(n+\tau)\, w_l^*(n+\tau)$. By considering that $w_{m,l}(n+\tau)$ and $w_l^*(n+\tau)$ are not only independent of each other but also follow a complex Gaussian distribution with mean zero and variance σ_w^2, and referring to the analysis results in Appendix, we can have that $W_{m,l}$ approximately obeys a complex Gaussian distribution with variance $N_{zc}\sigma_w^2$.

We define the sum of two complex Gaussian random variables $Q_{m,l} + X_{m,l}$ and $W_{m,l}$ in (17) as follows:

$$Y_{m,l} = Q_{m,l} + X_{m,l} + W_{m,l}. \tag{22}$$

Because the covariance between $Q_{m,l}+X_{m,l}$ and $W_{m,l}$ is 0, i.e.

$$Cov\left\{Q_{m,l}+X_{m,l},\, W_{m,l}\right\} = E\left\{\left(Q_{m,l}+X_{m,l}\right) W_{m,l}\right\} = 0, \tag{23}$$

where $Cov\{\cdot\}$ denotes the covariance operator, we can obtain that $Q_{m,l}+X_{m,l}$ and $W_{m,l}$ are uncorrelated. Further, since the uncorrelated complex Gaussian random variables are independent of each other, it immediately follows that the mean and variance of $Y_{m,l}$ are the summation of those of two terms, $Q_{m,l}+X_{m,l}$ and $W_{m,l}$, concretely, we have

$$E\{Y_{m,l}\} = E\{Q_{m,l}+X_{m,l}\} + E\{W_{m,l}\} = 0, \tag{24}$$

and

$$\begin{aligned} Var\{Y_{m,l}\} &= Var\{Q_{m,l}+X_{m,l}\} + Var\{W_{m,l}\} \\ &= N_{zc}\sigma_w^2(1+2\left|\rho\right|^2). \end{aligned} \tag{25}$$

Based on the above analysis, we have derived the statistical characteristics of the noise terms in (17) at the correct timing index. To further indicate the anti-noise capability of the proposed MSJC scheme, we compare the output power ratio of signal to noise, O_{PR}, for different number of sub-sequences involved in PDP calculation.

If $l = 1$, namely, only one sub-sequence is used in PDP calculation, $O_{PR}\left|_{l=1}\right.$ is expressed as

$$O_{PR}\left|_{l=1}\right. = \frac{E\left\{\left|P_{m,1}\right|^2\right\}}{E\left\{\left|Y_{m,1}\right|^2\right\}}. \tag{26}$$

When multiple sub-sequences are utilized, i.e. $l = l_0$ for $2 \le l_0 \le K$, $O_{PR}\left|_{l=l_0}\right.$ is given by

$$O_{PR}\left|_{l=l_0}\right. = \frac{E\left\{\left[\sum_{l=1}^{l_0}\left|P_{m,l}\right|\right]^2\right\}}{E\left\{\left[\sum_{l=1}^{l_0}\left|Y_{m,l}\right|\right]^2\right\}}. \tag{27}$$

Furthermore, we present to adopt the factor α to compare the output power ratio for different l, which can be defined as

$$\alpha = \frac{E\left\{\left[\sum_{l=1}^{l_0}\left|P_{m,l}\right|\right]^2\right\}}{E\left\{\left|P_{m,1}\right|^2\right\}} \Bigg/ \frac{E\left\{\left[\sum_{l=1}^{l_0}\left|Y_{m,l}\right|\right]^2\right\}}{E\left\{\left|Y_{m,1}\right|^2\right\}}. \tag{28}$$

It can be summarized from (28) that factor α depends on both the ratio of signal power ratio and noise power ratio for different l.

First, we focus on the derivation of signal power ratio. Since

$$E\left\{\left[\sum_{l=1}^{l_0}\left|P_{m,l}\right|\right]^2\right\} = \left[\left|\rho\right|^2\sum_{l=1}^{l_0}N_{zc}\right]^2 \tag{29}$$

and

$$E\left\{\left|P_{m,1}\right|^2\right\} = \left[\left|\rho\right|^2 N_{zc}\right]^2 \tag{30}$$

always holds, we can obtain that the signal power ratio that

$$\frac{E\left\{\left[\sum_{l=1}^{l_0}\left|P_{m,l}\right|\right]^2\right\}}{E\left\{\left|P_{m,1}\right|^2\right\}} = l_0^2. \tag{31}$$

Next, by considering the fact that the noise terms $Y_{m,l}$ for different l are independent of each other, the noise power ratio can be rewritten as

$$\begin{aligned} &\frac{E\left\{\left[\sum_{l=1}^{l_0}\left|Y_{m,l}\right|\right]^2\right\}}{E\left\{\left|Y_{m,1}\right|^2\right\}} \\ &= \frac{\sum_{l=1}^{l_0}E\left\{\left|Y_{m,l}\right|^2\right\}}{E\left\{\left|Y_{m,1}\right|^2\right\}} + \frac{\sum_{l=1}^{l_0}\sum_{j=1,j\neq l}^{l_0}E\left\{\left|Y_{m,l}\right|\right\}E\left\{\left|Y_{m,j}\right|\right\}}{E\left\{\left|Y_{m,1}\right|^2\right\}} \end{aligned} \tag{32}$$

It is noteworthy that $Y_{m,l}$ is a complex Gaussian random variable, and thus $\left|Y_{m,l}\right|$ follows a Rayleigh distribution with mean

$$E\left\{\left|Y_{m,l}\right|\right\} = \sqrt{\frac{\pi}{2}\left(\frac{Var\left\{Y_{m,l}\right\}}{2}\right)} \tag{33}$$

and variance

$$Var\left\{\left|Y_{m,l}\right|\right\} = \frac{4-\pi}{2}\left(\frac{Var\left\{Y_{m,l}\right\}}{2}\right). \tag{34}$$

Considering the relationship between mean and variance of the Rayleigh random variable, we can obtain that

$$E\left\{\left|Y_{m,l}\right|^2\right\} = \left[E\left\{\left|Y_{m,l}\right|\right\}\right]^2 + Var\left\{\left|Y_{m,l}\right|\right\} = Var\left\{Y_{m,l}\right\}. \tag{35}$$

Hence, the first term on the right side of (32) becomes

$$\frac{\sum_{l=1}^{l_0}E\left\{\left|Y_{m,l}\right|^2\right\}}{E\left\{\left|Y_{m,1}\right|^2\right\}} = \frac{\sum_{l=1}^{l_0}Var\left\{Y_{m,l}\right\}}{Var\left\{Y_{m,1}\right\}} = l_0. \tag{36}$$

On the other hand, the second term on the right side of (32) can be derived as

$$\begin{aligned} &\frac{\sum_{l=1}^{l_0}\sum_{j=1,j\neq l}^{l_0}E\left\{\left|Y_{m,l}\right|\right\}E\left\{\left|Y_{m,j}\right|\right\}}{E\left\{\left|Y_{m,1}\right|^2\right\}} \\ &= \frac{\sum_{l=1}^{l_0}\sum_{j=1,j\neq l}^{l_0}\sqrt{\frac{\pi}{2}\left(\frac{Var\{Y_{m,l}\}}{2}\right)}\sqrt{\frac{\pi}{2}\left(\frac{Var\{Y_{m,j}\}}{2}\right)}}{Var\left\{Y_{m,1}\right\}} \end{aligned}$$

$$= \frac{\pi}{4} \frac{\sum_{l=1}^{l_0} \sum_{j=1, j\neq l}^{l_0} \sqrt{Var\left\{Y_{m,l}\right\} Var\left\{Y_{m,j}\right\}}}{Var\left\{Y_{m,1}\right\}}$$
$$= \frac{\pi}{4} (l_0 - 1) l_0. \quad (37)$$

Consequently, submitting (36) and (37) to (32), we can obtain the noise power ratio as follows:

$$\frac{E\left\{\left[\sum_{l=1}^{l_0} \left|Y_{m,l}\right|\right]^2\right\}}{E\left\{\left|Y_{m,1}\right|^2\right\}} = l_0 + \frac{\pi}{4} (l_0 - 1) l_0. \quad (38)$$

Finally, the factor α can be determined as

$$\alpha = \frac{O_{PR}\left|_{l=l_0}\right.}{O_{PR}\left|_{l=1}\right.} = \frac{1}{\frac{\pi}{4} + \frac{(1-\frac{\pi}{4})}{l_0}}. \quad (39)$$

We can conclude from (39) that the value of α is greater than one when $l_0 > 1$ and proportional to l_0, which means that the output power ratio of signal to noise increases with the growth of the number of subsequences involved in PDP calculation. That is to say, with the increment of the available number of subsequences, the proposed MSJC scheme can effectively suppress the adverse impact of noise on the timing detection.

C. COMPUTATIONAL COMPLEXITY

For the load-limited satellite receiver, on the premise of guaranteeing the acceptable timing estimation performance, the computational complexity of preamble detection method should be reduced as much as possible. From the aforementioned analysis, we can further enhance the timing detection accuracy of the proposed MSJC method by increasing the available number of sub-sequences, L. When L is set to be its maximum value K, the capability of mitigation of noise for our method can reach its optimum. However, with the increment of L, the complexity of correlation continuously increases.

To achieve the best trade-off between detection performance and complexity, we further propose a low-complexity PDP calculation to effectively reduce the computational load. Note that, when $L = K$, all the sub-sequences can be utilized for PDP calculation. In this case, the sliding correlation in (6) can be replaced by the periodic correlation, and consequently we can use the operation of inverse fast Fourier transform (IFFT) instead of the correlation calculation to further reduce the time of complex multiplications [22], i.e.

$$\mathbf{C^d} = \frac{1}{N_{zc}MK} \sum_{m=1}^{M} \left| IFFT\left(\mathbf{A_m^*} \circ \mathbf{B_m^d}\right)\right| \quad (40)$$

where $\mathbf{C^d}$ denotes the low-complexity PDP calculation, $\mathbf{A_m}$ and $\mathbf{B_m^d}$ are the frequency domain forms of $\mathbf{a_m}$ and $\mathbf{b_m^d}$, respectively. It is obvious that, by compared (40) with (6), there are total N_{zc} complex multiplications saved at each timing position d, which significantly enhances the computational efficiency of preamble detection for the load-limited satellite receiver.

TABLE 1. The system parameters for S-band LEO1200 based NTN.

Parameters	Configurations
Band	S-band
Carrier frequency	2 GHz
Satellite altitude	1200 km
Beam set	Sat-2
Elevation angle	45 degree
Max differential delay	1.7 ms
Max Doppler shift	40 KHz
RACH bandwidth	1.08 MHz
Sub-carrier interval	1.25 KHz
CP duration, T_{CP}	3.4 ms
Long sequence duration, T_{LS}	6.4 ms
Short sequence duration, T_{SEQ}	0.8 ms
Short sequence length, N_{ZC}	839
Root index, u	[1,839]
Number of short sequences, K	8
Number of available short sequences, L	[1,8]
Time of cyclic shift, M	7
Channel model	LoS channel

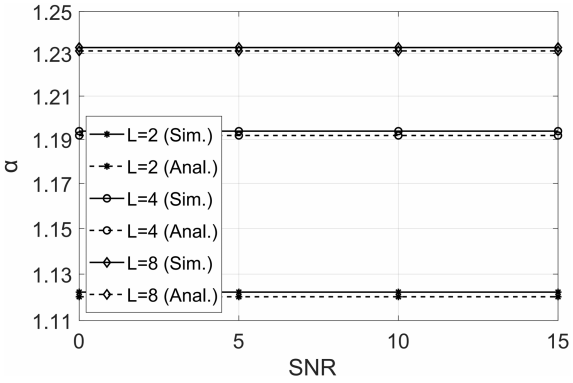

FIGURE 4. The values of factor α for different number of available sub-sequences.

V. NUMERICAL RESULTS

In this section, numerical results are explicitly given to demonstrate the performance improvement of the proposed preamble detection method by computer simulations. Table 1 lists the detailed system parameters for a typical LEO based NTN scenario, which has been adopted in 3GPP technical report 38.821 [17]. Note that, the performance comparisons with the two major solutions based on enhanced ZC sequence are not performed here, since their preamble sequences could be exactly represented by those in [13] and [15], respectively.

In Fig. 4, we illustrate the analytical and simulated values of the factor α versus SNR for different number of available sub-sequences, L. It is evident that the numerical results are almost the same as the theoretical results for different L, which verifies the validity of statistical analysis at the correct timing index for the proposed method. Here, the slight difference comes from the approximate derivation

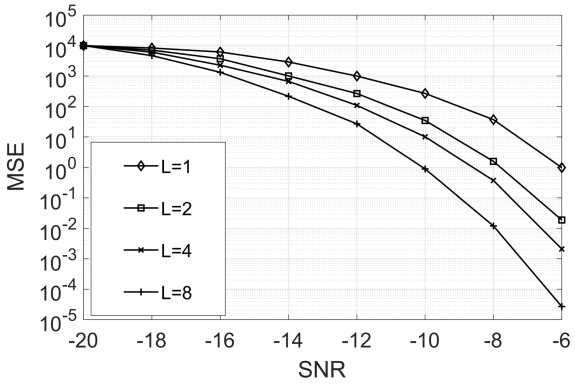

FIGURE 5. Timing estimation performance of the proposed method for different number of available sub-sequences.

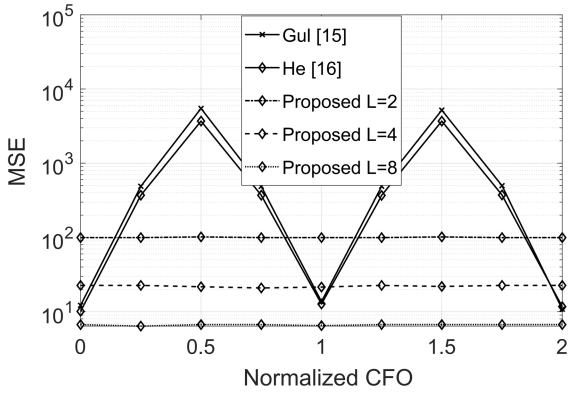

FIGURE 6. Timing MSE comparison of different methods versus normalized CFO.

of the probability distribution of the noise terms in (17). Note that, the value of α is independent of SNR and only increases with the increment of L, which is in line with the conclusion in (39), and demonstrate that increasing the number of available sub-sequences in PDP calculation can effectively enhance the noise-mitigation capability for the proposed MSJC.

In the following, we investigate the timing performance of the proposed approach for different L as shown in Fig. 5. The timing mean square error (MSE) is adopted as the criterion to evaluate the accuracy of timing estimation for different SNRs. It can be observed that the timing estimation error gradually reduces as the number of available sub-sequences L increases, and the performance gain between different L becomes higher with the increment of SNR. In other words, increasing L can significantly improve the timing estimation performance for the proposed method. However, computational complexity is also one of the important considerations in the practical implement. If the complexity is the main concern, we could choose relatively less sub-sequences in MSJC, e.g. $L = 1$ or $L = 2$; otherwise, we configure $L = 4$ or $L = 8$ to obtain a better timing performance than that of the former, when the system can afford such complexity.

Further, we make performance comparisons of the proposed approach with the related works. Fig. 6 depicts the timing MSE performance curves of various RA methods for different normalized CFOs, ε, at SNR $= -11$ dB. Note that, both methods in [15] and [16] achieve a relatively low timing MSE especially in the presence of integral ε, due to the conjugate symmetry of ZC sequences. Nevertheless, if the fractional ε exists, their timing estimation performance sharply degrade, which will obtain its worst case when the fractional ε is set to be the multiples of 0.5. On the contrary, the timing MSE performance of the proposed method remains nearly constant for different values of CFO, which indicates that the proposed MSJC is immune to CFO. This is because the adverse impact of large CFOs on timing estimation can be completely eliminated through the modulus operation of the correlation function in (17). Moreover, the timing estimation performance of our method can be further enhanced

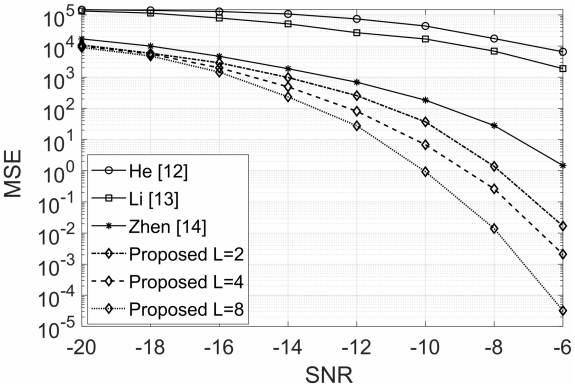

FIGURE 7. Timing MSE comparison of different RA methods versus SNR.

by increasing L, and remarkably outperforms the existing methods by setting $L = 8$.

Fig. 7 exhibits the timing estimation performance of various RA methods at different SNRs, wherein the normalized CFO is set to be 0.6. It is obvious in Fig. 7 that the method in [12] with small sub-carrier interval has a larger timing error at different SNRs, since its timing performance is greatly affected by CFO. The methods in [13] and [14] can reuse the terrestrial preamble format, but their performance of this method will degrade when the CFO is larger than half of the sub-carrier interval. In comparisons with these methods, our method that is capable of mitigation of noise can achieve a considerably lower MSE, due to the adjustable number of sub-sequences used in MSJC. Further, for saving the resource overhead, we can choose $L = 2$ with the guarantee of an acceptable timing estimation performance.

In addition, we also describe the error detection probabilities (EDPs) of different RA methods versus SNR in Fig. 8. Here, EDP represents the probability that the value of PDP at the correct timing point is lower than the preset detection threshold. For the lack of effective solutions either from the viewpoints of robustness to large CFOs or the mitigation of noise, all the methods in [12]–[14] have larger detection errors. It is clear that the proposed method obtains a significantly lower EDP compared to those of the previous methods,

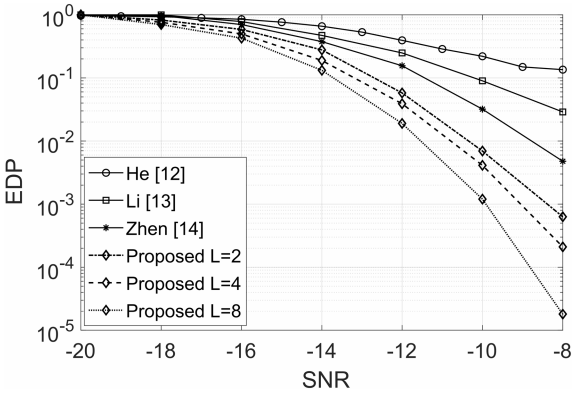

FIGURE 8. EDP comparison of different RA methods versus SNR.

and its detection performance can be further improved as L increases. Furthermore, in consideration of the detection performance requirement in 5G RA [23] (i.e. in the case that the false alarm probability is less than or equal to 0.1%, the corresponding error probability of detection for a single received antenna should be equal to or below 1% at SNR $= -11$ dB under an AWGN channel), we can choose $L = 8$ to effectively satisfy this target for realizing the 5G integrated satellite RA. In this case, the proposed low-complexity PDP calculation can be effectively utilized to further reduce the computational load.

VI. CONCLUSION

In this paper, we investigate the design and detection of random access preamble in 5G based satellite communication systems. A preamble sequence, MR-CLS, is first presented by concatenating multiple different root ZC sequences with large sub-carrier interval, by considering the system compatibility and characteristics of satellite environment. Meanwhile, the corresponding timing detection scheme, MSJC, is also proposed for one-step TA estimation, which can not only improve the access efficiency, but also extremely restrain the adverse impact of large CFOs and noise on timing estimation. Simulation results are consistent with mathematical analysis, and reveal the performance enhancement of the proposed method in a typical LEO based NTN scenario, compared to the related works. Furthermore, the proposed method can be applied to the most satellite RA scenarios, with no need for performing the pre-compensation of timing and frequency offset.

APPENDIX
STATISTICAL PROPERTIES OF CORRELATION FUNCTION AT THE WRONG TIMING INDEX

This section is dedicated to the statistical distribution derivation for the correlation function $corr_{m,l}(d_f)$ at the wrong timing position. Considering that the two noise terms, i.e. $w_l^*\left(n+d_f\right)$ and $w_{m,l}\left(n+d_f\right)$, are not only independent of each other but also both follow a complex Gaussian distribution with mean zero and variance σ_w^2, we respectively redefine them as

$$w_l^*\left(n+d_f\right) = T_1(n+d_f) - jU_1(n+d_f) \tag{41}$$

and

$$w_{m,l}\left(n+d_f\right) = T_2(n+d_f) + jU_2(n+d_f), \tag{42}$$

wherein $T_1(n+d_f) = Re\left\{w_l\left(n+d_f\right)\right\}$, $U_1(n+d_f) = Im\left\{w_l\left(n+d_f\right)\right\}$, $T_2(n+d_f) = Re\left\{w_{m,l}\left(n+d_f\right)\right\}$, $U_2(n+d_f) = Im\left\{w_{m,l}\left(n+d_f\right)\right\}$. Here, $Re\{\cdot\}$ and $Im\{\cdot\}$ denote the real part and the imaginary part of a complex random variable, respectively. Further, we can obtain that

$$E\left\{T_1(n+d_f)\right\} = E\left\{U_1(n+d_f)\right\} = \frac{E\left\{w_l^*\left(n+d_f\right)\right\}}{2} = 0, \tag{43}$$

$$E\left\{T_2(n+d_f)\right\} = E\left\{U_2(n+d_f)\right\} = \frac{E\left\{w_{m,l}\left(n+d_f\right)\right\}}{2} = 0, \tag{44}$$

$$Var\left\{T_2(n+d_f)\right\} = Var\left\{U_2(n+d_f)\right\} = \frac{Var\left\{w_{m,l}(n+d_f)\right\}}{2} = \frac{\sigma_w^2}{2}, \tag{45}$$

and

$$Var\left\{T_2(n+d_f)\right\} = Var\left\{U_2(n+d_f)\right\} = \frac{Var\left\{w_{m,l}\left(n+d_f\right)\right\}}{2} = \frac{\sigma_w^2}{2}. \tag{46}$$

Consequently, $corr_{m,l}\left(d_f\right)$ can be rewritten as

$$\begin{aligned} &corr\left(d_f\right) \\ &= \sum_{n=1}^{N_{zc}-1} ZC_l(n) ZC_{m,l}^*(n) \left[T_1\left(n+d_f\right) - jU_1\left(n+d_f\right)\right] \\ &\quad \times \left[T_2\left(n+d_f\right) + jU_2\left(n+d_f\right)\right]. \end{aligned} \tag{47}$$

For the convenience of discussion, we express $T_1(n+d_f)$ as T_1. Similarly, $T_2(n+d_f)$, $U_1(n+d_f)$, and $U_2(n+d_f)$ can be also represented as T_2, U_1, and U_2, respectively. It is worth noting that T_1, T_2, U_1, and U_2 are all the i.i.d. Gaussian random variables with mean zero and variance $\sigma_w^2/2$, respectively. Because the term $ZC_l(n) ZC_{m,l}^*(n)$ does not affect the statistical distribution of $corr_{m,l}\left(d_f\right)$, the mean and variance of $corr_{m,l}\left(d_f\right)$ can be given by

$$\begin{aligned} &E\left\{corr_{m,l}\left(d_f\right)\right\} \\ &= \sum_{n=1}^{N_{zc}-1} E\left\{\left(T_1 - jU_1\right)\left(T_2 + jU_2\right)\right\} \\ &= \sum_{n=1}^{N_{zc}-1} \left[E\left\{T_1T_2 + U_1U_2\right\} + E\left\{j(T_1U_2 - T_2U_1)\right\}\right] \\ &= \sum_{n=1}^{N_{zc}-1} \left[E\{T_1T_2\} + E\left\{U_1U_2\right\} + E\left\{T_1U_2\right\} - E\left\{T_2U_1\right\}\right], \end{aligned} \tag{48}$$

and

$$\begin{aligned} &Var\left\{corr_{m,l}\left(d_f\right)\right\} \\ &= \sum_{n=1}^{N_{zc}-1} Var\left\{\left(T_1 - jU_1\right)\left(T_2 + jU_2\right)\right\} \\ &= \sum_{n=1}^{N_{zc}-1} \left[Var\left\{T_1T_2 + U_1U_2\right\} + Var\left\{j(T_1U_2 - T_2U_1)\right\}\right. \\ &= \sum_{n=1}^{N_{zc}-1} \left[Var\left\{T_1T_2\right\} + Var\left\{U_1U_2\right\} + Var\left\{T_1U_2\right\}\right. \\ &\quad \left. + Var\left\{T_2U_1\right\} + Cov\left\{T_1T_2, U_1U_2\right\} - Cov\left\{T_1U_2, T_2U_1\right\}\right]. \end{aligned} \tag{49}$$

In [24], we can find the conclusion that the product of two i.i.d. Gaussian random variables is still approximately subject to a Gaussian distribution. Therefore, it can be obtained that T_1T_2, U_1U_2, T_1U_2 and T_2U_1 are still the Gaussian random variables, respectively, and thus their statistical properties can be achieved as

$$E\left\{T_1T_2\right\} = E\left\{U_1U_2\right\} = E\left\{T_1U_2\right\} = E\left\{T_2U_1\right\} = 0 \tag{50}$$

and

$$Var\{T_1T_2\} = Var\{U_1U_2\} = Var\{T_1U_2\} = Var\{T_2U_1\} = \frac{\sigma_w^2}{4}. \tag{51}$$

Meanwhile, we have

$$Cov\left\{T_1T_2, U_1U_2\right\} = Cov\left\{T_1U_2, T_2U_1\right\} = 0. \tag{52}$$

Finally, submitting (50) to (48) and bringing (51) and (52) into (49), respectively, it can be summarized that $corr_{m,l}(d_f)$ obeys a complex Gaussian distribution with mean zero and variance $N_{zc}\sigma_w^2$.

REFERENCES

[1] *Technical Specification Group Radio Access Network; Study on New Radio (NR) to Support Non-Terrestrial Networks; (Release 15)*, document 3GPP TR 38.811, 2019.

[2] M. De Sanctis, E. Cianca, G. Araniti, I. Bisio, and R. Prasad, "Satellite communications supporting Internet of remote things," *IEEE Internet Things J.*, vol. 3, no. 1, pp. 113–123, Feb. 2016.

[3] A. Guidotti, A. Vanelli-Coralli, M. Conti, S. Andrenacci, S. Chatzinotas, N. Maturo, B. Evans, A. Awoseyila, A. Ugolini, T. Foggi, L. Gaudio, N. Alagha, and S. Cioni, "Architectures and key technical challenges for 5G systems incorporating satellites," *IEEE Trans. Veh. Technol.*, vol. 68, no. 3, pp. 2624–2639, Mar. 2019.

[4] *Technical Specification Group Radio Access Network; NR; Physical Channels and Modulation; (Release 15)*, document 3GPP TS 38.211, 2018.

[5] Q. Xiong, B. Yu, C. Qian, X. Li, and C. Sun, "Random access preamble generation and procedure design for 5G-NR system," in *Proc. IEEE Globecom Workshops (GC Wkshps)*, Abu Dhabi, United Arab Emirates, Dec. 2018, pp. 1–7.

[6] G. Schreiber and M. Tavares, "5G new radio physical random access preamble design," in *Proc. IEEE 5G World Forum (5GWF)*, Silicon Valley, CA, USA, Jul. 2018, pp. 215–220.

[7] X. Lin, A. Adhikary, and Y.-P. Eric Wang, "Random access preamble design and detection for 3GPP narrowband IoT systems," *IEEE Wireless Commun. Lett.*, vol. 5, no. 6, pp. 640–643, Dec. 2016.

[8] J. Zou, H. Yu, W. Miao, and C. Jiang, "Packet-based preamble design for random access in massive IoT communication systems," *IEEE Access*, vol. 5, pp. 11759–11767, 2017.

[9] L. Siyang, Q. Fei, G. Zhen, Z. Yuan, and H. Yizhou, "LTE-satellite: Chinese proposal for satellite component of IMT-advanced system," *China Commun.*, vol. 10, no. 10, pp. 47–64, Oct. 2013.

[10] A. Guidotti, A. Vanelli-Coralli, M. Caus, J. Bas, G. Colavolpe, T. Foggi, S. Cioni, A. Modenini, and D. Tarchi, "Satellite-enabled LTE systems in LEO constellations," in *Proc. IEEE Int. Conf. Commun. Workshops (ICC Workshops)*, Paris, France, May 2017, pp. 876–881.

[11] S. Sesia, M. Baker, and I. Toufik, *LTE–The UMTS Long Term Evolution*. Hoboken, NJ, USA: Wiley, 2011.

[12] H. Yizhou, C. Gaofeng, L. Pengxu, C. Ruijun, and W. Weidong, "Random access preamble design based on time pre-compensation for LTE-satellite system," *J. China Univ. Posts Telecommun.*, vol. 22, no. 3, pp. 64–73, Jun. 2015.

[13] C. Li, H. Ba, H. Duan, Y. Gao, and J. Wu, "A two-step time delay difference estimation method for initial random access in satellite LTE system," in *Proc. 16th Int. Conf. Adv. Commun. Technol.*, Feb. 2014, pp. 10–13.

[14] L. Zhen, H. Qin, B. Song, R. Ding, X. Du, and M. Guizani, "Random access preamble design and detection for mobile satellite communication systems," *IEEE J. Sel. Areas Commun.*, vol. 36, no. 2, pp. 280–291, Feb. 2018.

[15] M. Muhammad Usman Gul, S. Lee, and X. Ma, "Robust synchronization for OFDM employing zadoff-chu sequence," in *Proc. 46th Annu. Conf. Inf. Sci. Syst. (CISS)*, Mar. 2012, pp. 1–6.

[16] H. Yizhou, C. Gaofeng, L. Pengxu, C. Ruijun, and W. Weidong, "Timing advanced estimation algorithm of low complexity based on DFT spectrum analysis for satellite system," *China Commun.*, vol. 12, no. 4, pp. 140–150, Apr. 2015.

[17] *Technical Specification Group Radio Access Network; Solutions for NR to Support Non-Terrestrial Networks (NTN)*, document 3GPP TR 38.821, 2019.

[18] B. Evans, O. Onireti, T. Spathopoulos, and M. A. Imran, "The role of satellites in 5G," in *Proc. 23rd Eur. Signal Process. Conf. (EUSIPCO)*, Aug. 2015, pp. 197–202.

[19] J. Hu and N. C. Beaulieu, "Accurate simple closed-form approximations to Rayleigh sum distributions and densities," *IEEE Commun. Lett.*, vol. 9, no. 2, pp. 109–111, Feb. 2005.

[20] G. K. Karagiannidis, T. A. Tsiftsis, and N. C. Sagias, "A closed-form upper-bound for the distribution of the weighted sum of Rayleigh variates," *IEEE Commun. Lett.*, vol. 9, no. 7, pp. 589–591, Jul. 2005.

[21] Z. Lin and Z. Bai, *Probability Inequalities*. China: Springer, 2011.

[22] *Physical Layer Aspects for Evolved Universal Terrestrial Radio Access (UTRA) (Release 7)*, document 3GPP TR 25.814, 2006.

[23] *Technical Specification Group Radio Access Network; NR; Base Station (BS) Radio Transmission and Reception (Release 16)*, document 3GPP TS 38.104, 2019.

[24] P. Bromiley, "Products and convolutions of Gaussian probability density functions," Tina-Vis. Memo, Univ. Manchester, Manchester, U.K., Internal Rep. 003-003, 2003, vol. 3, pp. 1–13.

[25] M. Hua, M. Wang, W. Yang, X. You, F. Shu, J. Wang, W. Sheng, and Q. Chen, "Analysis of the frequency offset effect on random access signals," *IEEE Trans. Commun.*, vol. 61, no. 11, pp. 4728–4740, Nov. 2013.

[26] M. Hua, M. Wang, K. W. Yang, and K. J. Zou, "Analysis of the frequency offset effect on Zadoff–Chu sequence timing performance," *IEEE Trans. Commun.*, vol. 62, no. 11, pp. 4024–4039, Nov. 2014.

[27] A. Papathanassiou, A. K. Salkintzis, and P. T. Mathiopoulos, "A comparison study of the uplink performance of W-CDMA and OFDM for mobile multimedia communications via LEO satellites," *IEEE Pers. Commun.*, vol. 8, no. 3, pp. 35–43, Jun. 2001.

LI ZHEN (Member, IEEE) received the M.S. degree in circuit and system from the Xi'an University of Posts and Telecommunications, Xi'an, China, in 2012, and the Ph.D. degree in communication and information systems from Xidian University, Xi'an, in 2018. He is currently with the School of Communication and Information Engineering, Xi'an University of Posts and Telecommunications. His research interests include weak signal detection and processing, random access, satellite mobile communications, and machine-type communications.

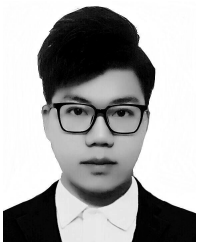

TENG SUN received the B.E. degree from the Shaanxi Sci-Tech University, Shaanxi, China, in 2017. He is currently pursuing the M.S. degree with the Xi'an University of Posts and Telecommunications, Xi'an, China. His current research interests include random access and 4G/5G satellite mobile communications.

GUANGYUE LU received the Ph.D. degree from Xidian University, Xi'an, China, in 1999. From 2004 to 2006, he was a Guest Researcher with the Signal and Systems Group, Uppsala University, Uppsala, Sweden. Since 2005, he has been a Professor with the Department of Telecommunications Engineering, Xi'an University of Posts and Telecommunications, Xi'an. His current research interests include signal processing in communication systems, cognitive radio, and spectrum sensing.

KEPING YU (Member, IEEE) received the M.E. and Ph.D. degrees from the Graduate School of Global Information and Telecommunication Studies, Waseda University, Tokyo, Japan, in 2012 and 2016, respectively. He was a Research Associate with the Global Information and Telecommunication Institute, Waseda University, from 2015 to 2019. He is currently a Junior Researcher with the Global Information and Telecommunication Institute, Waseda University. He has hosted and participated in a lot of research projects, including the Ministry of Internal Affairs and Communication (MIC) of Japan, the Ministry of Economy, Trade and Industry (METI) of Japan, the Japan Society for the Promotion of Science (JSPS), the Advanced Telecommunications Research Institute International (ATR) of Japan, the Keihin Electric Railway Corporation of Japan, and the Maspro Denkoh Corporation of Japan. He is also the Leader and a coauthor of the comprehensive book *Design and Implementation of Information-Centric Networking* (Cambridge University Press, 2020). He was involved in many standardization activities organized by ITU-T and ICNRG of IRTF, and contributed to the ITU-T Standards ITU-T Y.3071: Data Aware Networking (Information Centric Networking) Requirements and Capabilities and Y.3033-Data Aware Networking-Scenarios and Use Cases. His research interests include smart grids, information-centric networking, the Internet of Things, blockchain, and information security. He has had experience with editorial and conference organizations. He has served as a TPC Member of the IEEE VTC2019-Spring, ITU Kaleidoscope 2019, the IEEE HotICN 2019, the IEEE ICCC 2019, the IEEE WPMC 2019, EEI 2019, ICITVE 2019, the IEEE CCNC 2020, and the IEEE WCNC 2020. He is also an Editor of the IEEE Open Journal of Vehicular Technology (OJVT).

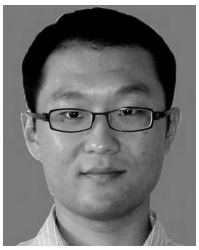

RUI DING received the B.S. and Ph.D. degrees in electronics and telecommunications from Southeast University, China, in 2001 and 2011, respectively. Since 2012, he has been a Senior Engineer with the China Academy of Space Technology, Beijing, China. His research interests include satellite communication systems and network design.